LA-UR-13-23344
Approved for public release; distribution is unlimited.

Title:	How to use the MCNP6 Background Source Capability
Author(s):	Fensin, Michael Lorne McKinney, Gregg W.
Intended for:	American Nuclear Society Winter Meeting, 2013-11-10/2013-11-14 (Washington, DC, District Of Columbia, United States)
Issued:	2013-05-08

How to use the MCNP6 Background Source Capability

M. L. Fensin and G. W. McKinney
Los Alamos National Laboratory, P.O. Box 1663 MS C921, Los Alamos, NM, 87545;
mfensin@lanl.gov and gwm@lanl.gov

INTRODUCTION

Many radiation detection applications for the Department of Homeland Security (DHS) involve trying to detect a minimum intensity source that is highly attenuated and within a small solid angle between source and detector. Further constraints involve optimizing timeliness of the detection scheme, as to not impede the flow of commerce, and minimization of the false positive detection rate.[1] Optimizing a detection strategy to meet these constraints involves examining hundreds to thousands of perturbations of conditions of operation (CONOPS). These perturbations, for particular CONOPS, may include: (1) swapping location of detection scheme (i.e. planes, trains, automobiles, boats, etc.); (2) altering orientation of detection equipment(s); (3) choice of detector technology; (4) choice of method for inducing source emission (active or passive); and/or (5) choice of source term. Modeling and simulation is ripe for initial investigation of down-selecting from these perturbations because it is cheap compared to building many instruments and setting up numerous detection schemes.

The MCNPX code, ending with MCNPX 2.7.0[2], contained several features developed for the Domestic Nuclear Detection Office (DNDO) to meet these simulation needs for DHS.[3] All features of MCNPX 2.7.0 were eventually merged into MCNP6;[4] therefore MCNPX or MCNP6 can simulate the: (1) complex 3D setups through the use of combinatorial geometry; (2) multi-particle emission signatures from passively decaying special nuclear material (SNM); (3) multi-particle emission signatures for active interrogation beams; (4) transport of multi-particle radiation through matter for wide ranging energies; (5) special purpose tallies to mimic the end-to-end behavior of the detector response; and (6) ability to trend the true positive versus false positive detection rate for a binary classifier system through use of Receiver-Operator Characteristic (ROC) curves.

A false positive detection event is caused by radiation whose origin is not from the SNM of interest, termed "background radiation". Background radiation has many sources: (1) cosmic rays that pass through the magnetosphere and interact in the upper atmosphere creating particles that match the particles trying to be detected; (2) **n**aturally **o**ccurring **r**adioactive **m**aterial (NORM) in the ground, water or surrounding structures that emit particles trying to be detected; and (3) other sources that are not the SNM of interest. In 2012, a cosmic ray source option was presented in MCNP6 that allowed users the capability to simulate a galactic cosmic ray (GCR) source spectrum (protons and alphas only) with proper magnetic rigidity, based on user provided location on the magnetosphere, and correct intensity and spectrum from solar modulation effects, based on a user provided date.[5] The GCR source could either be generated from the Lal analytic formulation with Energy Cutoffs (LEC)[6] or the Bartol Research Institute (BRI) formulation that used actual "sky-map" data.[7]

Also in 2012, a generic background source option was introduced that sampled neutrons and photons, from a background.dat source file, from one generic background source spectra from New York with scaling constants for neutrons on a 10^{o}X10^{o} longitude latitude grid around the world (assuming ground altitude).[5] In 2013, a second release of this file was presented containing actual spectra from around the world by simulating the GCR transport from the top of the atmosphere to the ground on a 10^{o}X10^{o} longitude/latitude grid around the world, and adding a generic terrestrial soil photon emission spectra (from K, U, Th, etc. decay).[8] This new release included not only air to ground transport effects but also ground reflection effects. Measured spectra taken at SNLL, Livermore, CA in 2006 compared nicely to newly simulated spectra.[8] Ref. 8 only focused on the generation of the new background.dat file. Using very simple geometry, this paper focuses specifically on considerations for using this new background source capability in typical MCNP simulations.

METHOD

The background source is intended to be used as a uniformly distributed source within a volume. For most applications, this volume will either be a cylinder, cube or sphere. If you start a uniform particle flux in a volume, the source strength must be renormalized in order to get a flux of 1 particle/cm^2-s at the geometric center of the volume. Therefore in order to get the proper magnitude of the background flux at the center of a particular volume, the user must adjust the magnitude of the background source. Fluxes can be adjusted by either: (1) post-processing; (2) 1^{st} entry on the fm card; or (3) setting the WGT keyword of the SDEF card. Since the background source is intended to be used with other beam sources, the best option is to set the WGT keyword on the SDEF card (except when used with the ROC feature – see more below).

This source renormalization is related to the leakage of the geometry and therefore related to the surface area

(SA) of the geometry. Several tests were completed, simulating a spatially uniform source within a void for various geometrical sizes of cubes, cylinders and spheres, to determine adequate normalization constants, in order to set the WGT keyword. The results were as follows: (1) for a cube, wgt = SA/~3.7 (ranged 3.65-3.73); (2) for a cylinder, wgt = SA/~3.4 (ranged 3.37-3.47); and (3) for a sphere, wgt = SA/~3.0 (ranged 2.93-3.0). These geometric divisors will be referred to as SD. MCNP is capable of simulating radiation transport to a point using an analytic scoring technique known as a point detector. A point detector tally is scored by $\frac{W*p(\mu)*e^{-\lambda}}{2\pi R^2}$; where W = particle weight, λ = mean free path, R = distance to detector and p(μ) = probability of scatter into the detector. In a void, $e^{-\lambda} = 1$. The uniformly distributed isotropic source can have starting histories that are sent in direct path of the detector, and as a result p(μ) can range significantly; therefore it can be quite difficult to converge a point detector result of this simulation. As a result, the simulations to generate the normalization constants used a volumetric flux tally (f4) on a small finite volume at the center of the geometry. The range of the above constants is due to the ability of the small finite volume to represent an actual point for various sizes of the full geometry.

Though the background source contains only induced neutron and photon particle fluxes at the ground altitude for given longitude and latitude, for most simulations these fluxes are all that you need for determining backgrounds related to these particles. For example, two MCNP6 cosmic ray simulations at 10 m above ground for Misawa, Japan and Los Alamos, NM were completed tracking neutrons (n), photons (p), protons (h), alphas (a), positive pions (/), deuterons (d), tritons (t), hellions (s), kaons (k), muons (|), neutral pions (z), anti-neutrons (q), anti-protons (g), positive muons (!), negative pions (*) and negative kaons (?). The downward directed particle current at Misawa Japan was 12.58% neutrons, 24.05% photons, 28.46% muons and 34.14% positive muons (antimuons). The downward directed particle current at Los Alamos, NM was 21.40% neutrons, 50.97% photons, 11.92% muons and 14.22% antimuons. The muon flux is wide ranging in energy; however, greater than ~57% of the muon and anti muon spectra are between 1-8 GeV. The ground-level muon spectra also has a ~cosine angular distribution (in 2π).

Four other simulations were also completed to compare the above ground neutron and photon spectra for Misawa, Japan and Los Alamos, NM assuming a 10 m ground depth of stainless steel with and without perfect muon absorption. The simulation ground was chosen to represent a worst case scenario of muon and antimoun based neutron and photon production that could be emitted back into the background volume. For Los Alamos, NM, when muon transport was turned off in the ground, the energy integrated neutron flux was only 3.97% lower and the energy integrated photon flux was only 1.46% lower. For Misawa, Japan, when muon transport was turned off in the ground, the energy integrated neutron flux was only 11.37% lower and the energy integrated photon flux was only 4% lower. It is important to note for the background source that though the energy integrated flux statistical error for neutrons and photons is less than a few percent, the error per energy bin ranges between 10-30%. Therefore the lack of muon and antimuon presence in the background source has minimal impact for simulations not containing significant stainless steel structures.

Though there are muon cross sections for nuclear interaction, these cross sections are in the nanobarn regime. Therefore muon capture is really dictated by orbital capture. When the muon slows down, it can be captured in the muon shell structure. As the muon migrates from the outer shells to the ground-state shell, the muon emits x-rays, just like electrons only with much higher energy and then cascade down to the 1s level emitting Auger electrons and X-rays. When the muon is in the 1s ground state the orbital radius approaches the nuclear radius, and because of the weight of the muon, the muon can deliver between 10-20 MeV of excitation energy to the nucleus (the muon can also decay while in orbit and not necessarily deliver its energy to the nucleus), which is well above the ~8 MeV required to emit a neutron.[9] Unlike muons, antimuons (positive muons) are repelled from the atomic nucleus and therefore are not captured. Therefore antimuons simply decay in-flight creating positrons that annihilate to produce photons.

The background source capability is intended for only air over ground/water and should not be used when other significant structures are present (large buildings, mountains, large chunks of concrete, etc.). If significant structures are present it is recommended to transport a full cosmic source as the muon effect could be as large as a few percent.

The background spectra can be counted in a typical detection scenario using various FT treatments to mimic the detector setup. For example, we could compose a cell of germanium and use a pulse height tally (f8) in combination with an FT GEB treatment to mimic the Gaussian energy broadening within the detection cell for a typical high purity germanium (HPGE) detector. We could also use a pulse height light (PHL) tally to accumulate the energy deposition of the charged particles created from a neutron capture event, like in a He-3 detector. However, the background source really gets its strength when used in combination with an interrogation source to generated ROC curves through use the FT ROC treatment. The FT ROC treatment was introduced in MCNPX 2.7.D (as a result is also available in MCNP6).[10] A user can define an interrogation source (or passive emission spectra of a source object) and then define a background source on an SDEF card, where the particle type definitions of the background source and interrogation source must be placed within the same

distribution number. The user would then specify FTn SCX m ROC A. Where n is the tally number; m is SI distribution number containing the background and interrogation particle declarations; and A is the total number of particles emitted during the time of interest, so after running this number of particles MCNP6 can deduce the total detector counts for that batch. After hundreds of batches, it can then form the detector count probability distribution function or PDF (i.e., probability vs total counts). The SCX m splits the contributions of a particular tally based on the user bins from the SDEF SI distribution number m. Scores for tally n are binned according to which source distribution m the source particle came from.[3]

The ROC treatment separates a tally into signal (interrogation source) and noise (background source). The signal and noise tally values are saved for batches of histories. The distribution of scores across a sample of batches is used to form signal and noise PDFs. The integration of the signal PDF is plotted as a function of the integral of the noise PDF resulting in the printed ROC curve. Entries 1-8 of the TF card are used to specify the signal bins of the tally and entries 9-16 are used for the noise portion. It is recommended to set the total number of particles such that there are at least 50-100 batches to analyze in generating the ROC curve.[3] When using ROC curves, it is important to turn off all non-analog transport (i.e. also set SDEF WGT=1), and use tallies that represent a binary effect (i.e. weight/no weight (f1) or pluses/no pulses (FT PHL)). The first production release of MCNP6 does not allow FT ROC with f8 tallies; however, the FT PHL tally is technically compatible with the FT ROC. Future production releases may likely support this combination of features.

The background source can emit neutrons only (bn), photons only (bp) or neutrons and photons (bg). If the user specifies bn, bp or bg for the PAR keyword the background spectra will be normalized to the correct magnitude for a given location using the LOC keyword (the user must still provide renormalization values mentioned before in order to get the correct magnitude across the geometry; the user should search the background.dat data file for a relevant longitude and latitude). If the values are negative the magnitude of the source strength is not readjusted. When trying to use FT ROC, it may be easier to use a "-" background particle. For example, say we have a mixed source of bn + n. For a normal tally, the WGT should then be the total number of neutrons for a given detection time, or the total neutrons per second. Let's say we were interested in a location near New Orleans (30N 90W) where the bn flux is 0.017 n/cm^2-s (we would look up this value in the background.dat), which corresponds to a source strength of 0.017*SA/SD n/s (where SD is the divisor coefficient mentioned above) and the n source strength was 1e6 n/s. The SDEF card would then be

```
SDEF … PAR=D1 WGT=0.017*SA/SD+1e6 LOC=30 -90 0
SI1 L          -bn                                  n
SP1 (0.017*SA/SD)/(0.017*SA/SD+1e6)  1e6/0.017*SA/SD+1e6)
```

However, when using FT ROC, the WGT must be set to 1 and analog transport must turned on by using cut:<pl> 2j 0 0 (cut:n 2j 0 0 for our example). The SDEF card now becomes

```
SDEF … PAR=D1 WGT=1 LOC=30 -90 0
SI1 L          -bn                                  n
SP1 (0.017*SA/SD)/(0.017*SA/SD+1e6)  1e6/(0.017*SA/SD+1e6)
```

The FT ROC A value is now set to (0.017*SA/SD+1e6)*t; where t is the count time for the detection.

RESULTS

Using our New Orleans example, we will generate a ROC curve for a simple detection scenario involving detecting neutrons from a 5 kg sphere of depleted uranium (DU) using a 2 MeV neutron interrogation source at 1e3 n/s. The DU will either be surrounded by 6 cm of borated polyethylene (shielded) or nothing (unshielded). In many cases, shielding is placed around the detector to improve probability of detection (PD) versus probability of false alarm (PFA). The example presented here shows the relative difficulty in detection for shielded versus unshielded DU. The detector will be 1 cm in radius and located 30 cm above the center of the DU. Before dismissing the geometry as unrealistic, we could imagine that our model is assuming the source was already highly attenuated before reaching the borated poly, and a handheld detector is placed a certain distance away from the object.

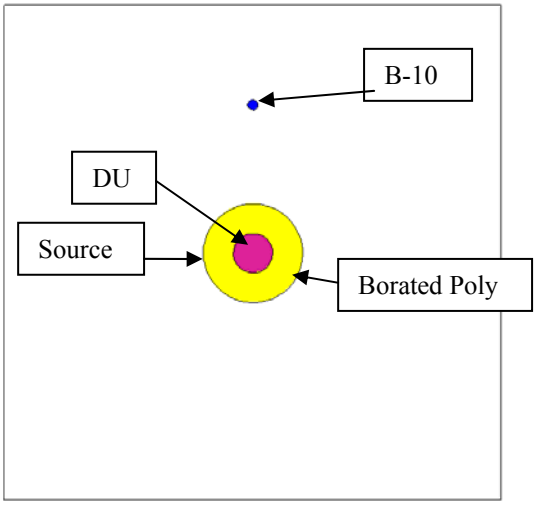

Fig 1. DU Sphere with B-10 detector setup.

The detector will be composed of 100% B-10. When B-10 absorbs a neutron, the compound nucleus is left with

enough energy to emit an alpha leaving a residual Li-7 nucleus. Both the alpha and Li-7 are left in a charged state; therefore it is these particles that cause ionizations as these particles slow down in the detector volume (or B-10 in our example). The energy deposition from these particles in the detector volume is very quick; hence an actual detector will only register the sum of the energy deposition events from these particles. The FT PHL tally treatment allows the capability to register the sum energy deposition from multiple particles, from the same starting history, that traverse a particular volume (surface-to-surface crossings in a volume).

Fig. 1 displays the geometry setup, which is centered at (0, 0, 0). The background volume is a 1 m cube. Therefore SD = 3.7 and SA = 6e4. The corresponding SP value for the -bn SI entry is (0.017*6e4/3.7)/(0.017*6e4/3.7 + 1e3) = 0.2161, and the corresponding SP value for the n SI entry is 1e3/(0.017*6e4/3.7+1e3) = 0.7839. The interrogation source will be a pencil beam point source located just outside the radius of the DU sphere at (-9.98, 0, 0) heading directly toward the center of the DU sphere. Therefore the SDEF card becomes

```
SDEF  PAR=D1 WGT=1 X=FPAR=D2 Y=FPAR=D3
      Z=FPAR=D4 VEC=FPAR=D5 DIR=FPAR=D6
      ERG=FPAR=D7 LOC=30 -90 0
SI1 L       -bn            n
SP1       0.2161     0.7839
DS2  S      20       21
DS3  S      30       31
DS4  S      40       41
DS5  S       0       51
DS6  S       0       61
DS7  S       0       71
SI20       -49.99    49.99
SP20         0       1
SI21 L     -9.98
SP21         1
SI30       -49.99    49.99
SP30         0       1
SI31 L       0
SP31         1
SI40       -49.99    49.99
SP40         0       1
SI41 L       0
SP41         1
SI51 L       1 0 0
SP51         1
SI61 L       1
SP61         1
SI71 L       2
SP71         1
```

We will simulate a 60s count time and use 500 batches to generate the signal and noise PDFs for the ROC curves. These parameters result in an FT ROC A value of 76540 and an nps of 3.827e7. For real production simulations, more batches may be required. For a normal current (f1) tally, the signal vs. noise components can easily be segregated using SCX before the ROC entries. For example, if using and f1 tally where si1 was the particle distributions for signal and noise, the ROC curve could be generated by FT1 scx 1 ROC 7.656e4; where the TF card becomes tf4 j j 2 j j j j j j j 1 j j j j j. Unfortunately, an f1 tally by itself only computes total number of particles crossing a surface and does not directly compute captures in B-10. We could augment the f1 tally by adding cosine bins (c1 0 1 T) and applying cosine multipliers (cm1 1 -1). The cosine multipliers would cause the total cosine bin (T) to contain the subtraction of the outgoing number of particles from the incoming number of particles (or number of captures in the volume per history). The TF card would now become tf4 j j 2 j j 3 j j j j 1 j j 3 j j to use the correct cosine bins of the f1 tally; however, these f1 tallies only consider the neutron capture and do not account for how the energy is deposited in the detector volume.

The FT PHL is a special pulse height tally (PHT) treatment that combines energy deposition events recorded in separate f6 tallies. The FT PHL treatment is not only capable of combining energy deposition from several f6 tallies but can also examine the coincidence/anticoincidence from groupings of f6 tallies. We leverage this coincidence/anticoincidence with the SCX treatment in order to segregate the Li-7 and alpha energy depositions from signal versus noise. To accomplish this task first we generate two sets of identical f6 tallies. Assuming cell 2 is the volume of the energy deposition location, we add the following f6 tallies

```
f6:a 2
f16:# 2
f26:a 2
f36:# 2
```

We then add an FT6 SCX treatment, for each tally, to segregate the contribution of signal and noise for each f6 tally. Next we add a tally fluctuation (TF) card for each f6 tally to assure that the tally information that is sent to the FT PHL is computed for the correct signal or noise user bin of the SCX treatment resulting in the following tally cards

```
f6:a 2
ft6  scx 1
tf6 1 j 1 j j j j j
f16:# 2
ft16 scx 1
tf16 1 j 1 j j j j j
f26:a 2
ft26 scx 1
tf26 1 j 2 j j j j j
f36:# 2
ft36 scx 1
```

```
tf36 1 j 2 j j j j j
```

At first, the inclusion of these two sets of alpha and Li-7 tallies (Li-7 is grouped with all heavy ions as the "#" particle) may seem redundant; however, we then use the important user bins (signal versus noise components of SCX) to construct the FT PHL tally by the following

```
f8:n 2
ft8  PHL 2   6 1 16 1
           2 26 1 36 1 0
e8  0 20
fu8 0 20
```

After the PHL, the first 2 dictates that two f6 tallies will be used to populate the 1st detector region for coincidence/anticoincidence detection. These two f6 tallies are tally 6 and 16. The 1 following the 6 entry tells MCNP to use the first f-bin (because we only specified 1 cell per f6 tally – cell 2 – there is only 1 f-bin number for each f6 tally). Detector region 2 is composed of the 1st f-bin from tallies f26 and f36.

The energy bins (e8) and tally user bins (fu8) are used to set energy discrimination for computing the coincidence/anticoincidence. The first energy bin (0) combined with the first user bin (0) represents the fraction of histories where no energy is deposited in either region (i.e., no neutron captured from bn or n). The first energy bin (0) combined with the second user bin ($0<E_2\leq 20$ MeV) represents the fraction of histories where energy is deposited only in region 2 (i.e., neutron capture from n). The second energy bin ($0<E_1\leq 20$ MeV) combined with the first user bin (0) represents the fraction of histories where energy is deposited only in region 1 (i.e., neutron capture from bn). And finally, the second energy bin ($0<E_1\leq 20$ MeV) combined with the second user bin ($0<E_2\leq 20$ MeV) represents the fraction of histories where energy is deposited in both regions (i.e., neutron capture from both bn and n – which should never occur). It is important to notice that we have segregated the detector regions, using SCX and TF cards, to be composed only of signal or noise; therefore there is no chance of coincidence events as MCNP either emits the bn source or the n source.

To complete our tally cards we now add the ROC treatment to the FT card after the PHL entries as well as a TF card for the entire f8 tally in order to tell the ROC treatment which tally results to employ as such

```
ft6  scx 1
tf6 1 j 1 j j j j j
f16:# 2
ft16 scx 1
tf16 1 j 1 j j j j j
f26:a 2
ft26 scx 1
tf26 1 j 2 j j j j j
f36:# 2
ft36 scx 1
tf36 1 j 2 j j j j j
f8:n 2
ft8   PHL 2   6 1 16 1
            2 26 1 36 1 0
      ROC 76560 500
e8  0 20
Fu8 0 20
tf8  j j 2 j j j 1 j
     j j 1 j j j 2 j
```

Though the FT ROC entries would be the same for either an f8 or f1 tally, the TF8 card entries are much more complex than the related TF1 entries would be. For our example, the first user bin of SCX is bn and the second is n; therefore f6 and f16 correspond to bn (PHL region 1) and f26 and f36 correspond to n (PHL region 2). Thus bn contributions are associated with E-bins and n contributions with U-bins, which means the first set of 8 entries on the TF8 card (i.e., signal bins) should point to the 1st E-bin and the 2nd U-bin and the second set of 8 entries (i.e., noise bins) should point to the 2nd E-bin and 1st U-bin.

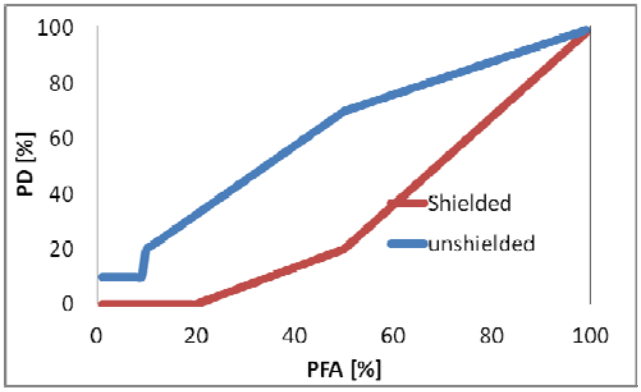

Fig 2. ROC Curve for detection scenario.

Fig. 2 presents the ROC curve generated from the simulation. Due to the fact that the simulation did not involve many histories, the ROC curve does not have a converged shape. Nonetheless the curve is very instructive in its own right. For example, in order to have a PFA close to 0%, the unshielded scenario only then has a PD of ~10%. This is probably due to the fact that the shielding attenuates the source and scattered/emitted signal from the DU. Due to the size of the detector and distance from DU (small solid angle), it is not possible for the source to overwhelm the background. If the detector was larger and closer to the DU, the larger solid angle of direct scatter/emission into the detector would increase the PD versus PFA. If the DU is unshielded, then there exists a large probability that source will cause enough fissions in the DU to make the signal from the source clearly overwhelm the signal from the background. It is

important to realize that solid angle is important and not the size of the detector. For example, if the detector was larger but placed further from the source, and the source was isotropic, the source may have fewer interactions per emission with the detector while the background would have more interactions with the detector increasing the PFA vs. PD.

CONCLUSIONS

MCNP continues to be a key DHS simulation tool for SNM detection. A new background source capability is available in MCNP6 on a $10^{o}X10^{o}$ longitude/latitude grid around the world (assuming ground altitude). The background source is composed of neutrons and photons only; however, based on how the source was generated, the lack of muon and antimuon inclusion in the background source file is sufficient for most air over ground/water simulations not using significant steel structures. The user can select to use neutrons, photons or a combination of both particles by setting par equal to bn, bp or bg. If the particle type is positive then the spectra magnitudes are adjusted automatically to match magnetic rigidity effects around the globe. If the particle specifications are negative, these adjustments are not automatically added. To use the background source for normal tallies, the user must readjust the WGT keyword on SDEF card based on the SA and SD for a particular background volume (recommended values for SD were presented). For FT ROC tallies, analog transport must be used and therefore the SDEF WGT is set to 1. The FT ROC A value is set to the product of the background particle normalization constant, SA and t divided by SD. An example problem was specified in order to help users implement this capability in a typical detection scenario, and an example ROC curve is provided.

ENDNOTES

This work was sponsored by the US Department of Homeland Security, Domestic Nuclear Detection Office, under competitively awarded contract/IAA HSHQDC-12-X-00251. This support does not constitute an express or implied endorsement on the part of the Government.

REFERENCES

1. http://www.dhs.gov/shielded-nuclear-alarm-resolution-snar
2. D. B. PELOWITZ, editor," MCNPX User's Manual Version 2.7.0," *LA-CP-11-00438* (2011).
3. http://www.fas.org/sgp/crs/nuke/RL34574.pdf
4. T. GOORLEY, M. James, T. Booth, F. Brown, J. Bull, L. J. Cox, J. Durkee, J. Elson, M. Fensin, R.A. Forster, J. Hendricks, H.G. Hughes, R. Johns, B. Kiedrowski, R. Martz, S. Mashnik, G. McKinney, D. Pelowitz, R. Prael, J. Sweezy, L. Waters, T. Wilcox, T. Zukaitis, " Initial MCNP6 Release Overview: MCNP6 version 1.0," *Journal of Nuclear Technology*, **180**, pg. 298-315 (2012).
5. G. W. MCKINNEY, H. J. Armstrong, M. R. James, J. M. Clem, and P. Goldhagen, "MCNP6 Cosmic-Source Option," *Trans ANS Annual Meeting*, Chicago, IL (2012).
6. G. C. CASTAGNOLI and D. LAL, "Solar Modulation Effects in Terrestrial Production of Carbon-14," *Radiocarbon*, **22**, No. 2, 133-158 (1980).
7. J. M. CLEM, G. DE ANGELIS, P. GOLDHAGEN, and J. W. WILSON, "New Calculations of the Atmospheric Cosmic Radiation Field – Results for Neutron Spectra," *Radiation Protection Dosimetry*, **110**, pp. 423-428 (2004).
8. J. PALOMARES, G. W. McKinney, "MCNP Simulations of Background Particle Fluxes from Galactic Cosmic Rays," *Trans. ANS Annual Meeting*, Atlanta, GA (2013).
9. D. F. MEASDAY, "The nuclear physics of muon capture," *Physics Reports*, **354**, pg. 243–409 (2001).
10. D. B. PELOWITZ, J. W. Durkee, J. S. Elson, M. L. Fensin, J. S. Hendricks, M. R. James, Russell C. Johns, G. W. McKinney, S. G. Mashnik, J. M. Verbeke, L. S. Waters, "MCNPX 2.7.D Extensions," LA-UR-10-07031 (October 20, 2010).